

# Backstepping and flatness approaches for stabilization of the stick-slip phenomenon for drilling

C. Sagert\* F. Di Meglio\* M. Krstic\* P. Rouchon\*\*

\* Department of Mechanical and Aerospace Engineering, University of California San Diego, La Jolla, CA 92093-0411, USA.

\*\* Centre Automatique et Systèmes, MINES ParisTech, 60, Bd St-Michel, 75272 Paris, Cedex 06, France.

**Abstract:** In this article, we propose control solutions to suppress undesirable torsional oscillations of the drill string in oil well drilling systems. Two feedback control laws are derived from Partial Differential Equations (PDE) models capturing the main features of the so-called stick-slip phenomenon. Comparative simulations highlight the merits of the two approaches.

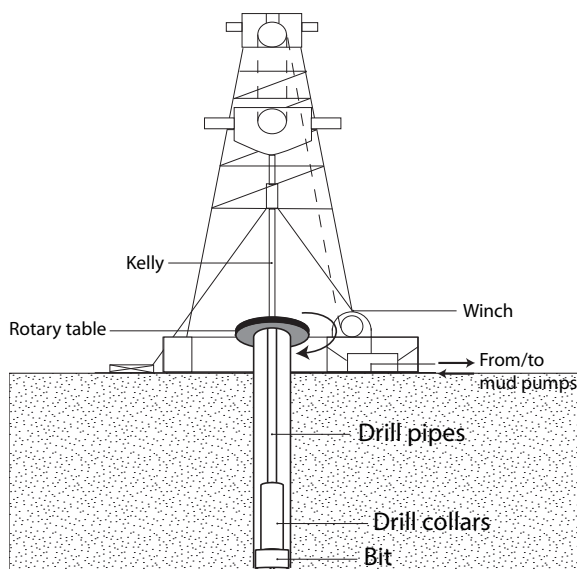


Fig. 1. Schematic view of a drilling system.

## 1. INTRODUCTION

The process of oil well drilling consists in the creation of a borehole several hundred meters deep in the ground until an oil reservoir is reached. The drillstring, consisting of the assembly of drill pipes, drill collars, and the rock-cutting tool referred to as drill bit (see Figure 1) rotates around its vertical axis, penetrating through the rock. At the top of the drillstring, the rotary table provides the necessary torque to put the system into a rotary motion. The drillstring is subject to three main types of instabilities, as described in Jansen (1993): Vertical vibrations, leading to pressure oscillations in the mud, whirl oscillations, due to an imbalanced drillstring, and torsional vibrations, corresponding to stick-slip oscillations. In this article, we propose solutions to suppress the latter.

Stick-slip oscillations are the result of specific downhole conditions, such as particular rock composition or small diameter of the borehole. These can cause the bit to stall, while the rotary table is still in motion. When enough energy has accumulated, the bit is suddenly released and starts rotating at very high

velocities, before friction slows it down and causes it to stall again. The resulting limit cycle leads to important damage on the facilities, and negatively impacts the rate of penetration<sup>1</sup> of the drilling system.

The torsional dynamics of the drillstring are governed by a wave equation (see, e.g., Balanov et al. (2003)). However, most of the literature on the stick-slip phenomenon relies on finite dimensional models, where the wave equation is replaced by a torsional spring<sup>2</sup>. This simplification allows the authors to apply classical control strategies to suppress the stick-slip oscillations: in Jansen (1993), a frequency-domain analysis leads to the design of a band-pass filter for the average rotary speed of the drillstring; in Navarro-Lopez and Cortes (2007) a sliding-mode controller based on a 7-state nonlinear model is derived; in Serrarens et al. (1998), an  $\mathcal{H}_\infty$  controller is proposed, based on a linearized 2-state model. However, these approaches neglect the time delay needed by the torsional waves to propagate in the material, which for long drillstrings may lead to undesirable effects.

In this article, we design controllers for the infinite dimensional wave equation, where the nonlinear dry friction term appears at the bottom boundary condition, similarly to Saldívar et al. (2011). The control objective is to operate at a constant uniform rotary speed. However, as will appear, for some values of the reference velocities, the corresponding trajectory is unstable, with infinitely many eigenvalues in the right-half plane. To stabilize such trajectories, we propose two distinct approaches, based on two approximations of the simulation model.

In our first approach, we neglect in-domain friction and the inertia of the drill bit. Exploiting the flatness property of the system (see, e.g. Fliess et al. (1993); Petit and Rouchon (2002)), we design a stabilizing controller relying on a sole measurement of the topside velocity. The feedback law takes the form of a nonlinear Proportional-Integrator (PI) with distributed delays.

In our second approach, following Smyshlyaev and Krstic (2009) and Krstic (2009a,b), we design a backstepping con-

<sup>1</sup> i.e., the vertical downward speed.

<sup>2</sup> Actually, several cascaded torsional springs corresponding to the drill pipes, drill collars and drill bit are often considered.

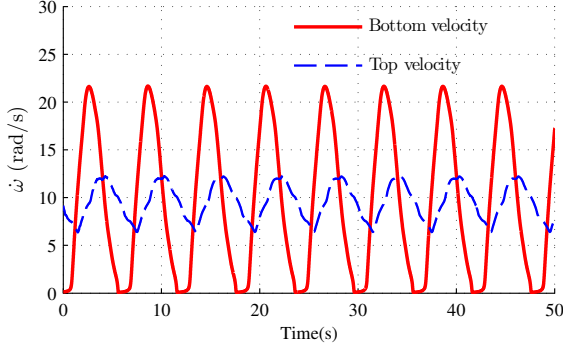


Fig. 2. Simulations of the stick-slip oscillations

troller for the linearized model around a reference trajectory. The controller is designed by putting the system under the form of an wave equation coupled, at the boundary, with an unstable Ordinary Differential Equation (ODE) describing the dynamics of the drill bit. Mapping the resulting equations to a target system with desirable stability properties, we derive a full-state feedback control law.

The article is organized as follows. In Section 2 we describe the system and the model equations. In Section 3 and 4 we derive two control laws based on the flatness property of the system and a backstepping approach. Section 5 illustrates the relevance and merits of both approaches in numerical simulations.

## 2. SYSTEM DESCRIPTION AND MODELLING

We consider the torsion dynamics of an oil well drillstring, pictured on Figure 1. Following Saldívar et al. (2011), after normalization, the angular displacement  $u(x, t)$  satisfies the following wave equation with boundary conditions with boundary conditions

$$u_{tt}(x, t) = u_{xx}(x, t) - \lambda u_t(x, t), \quad x \in [0, 1], t > 0 \quad (1)$$

$$u_x(1, t) = U(t) \quad (2)$$

$$u_{tt}(0, t) = a u_x(0, t) + a F(u_t(0, t)) \quad (3)$$

The boundary condition (2) represents the torque actuation from the rotary table at the topside boundary where  $U(t)$  is the control input. Equation (3) models the drill bit dynamics,  $u_t(0, t)$  being the bit rotary speed. The nonlinear function  $F$ , representing the rock-on-bit friction, is assumed to be perfectly known<sup>3</sup>. In this paper, we focus on trajectories of (1)–(3) corresponding to a uniform constant rotary speed  $\bar{u}_t(x, t) \equiv \omega_r$ , i.e. trajectories of the form

$$\bar{u}(x, t) = \frac{\lambda \omega_r}{2} x^2 - F(\omega_r)x + \omega_r t + u_0 \quad (4)$$

with the following reference control input

$$\bar{U} = \lambda \omega_r - F(\omega_r) \quad (5)$$

For certain values of  $\omega_r$ , these can be unstable: linearizing Equations (1)–(3) around such a trajectory, one can numerically compute the eigenvalues of the system, which are all located in the right-half-plane for large values of  $a$  (see, e.g., Krstić (2009a)). The solutions of the nonlinear system (1)–(3) then converge to a limit cycle, corresponding to large oscillations of the rotary speed of the drill bit. These oscillations, pictured on Figure 2, are detrimental to the drilling process. We propose

<sup>3</sup> In practice, the function  $F$  depends on the nature of the rock, which is not only poorly known but varying, as well as the weight-on-bit, which also varies during the course of a drilling operation.

to suppress them by stabilizing the trajectories of the form (4)–(5). Our first approach, detailed in the next section, consists in exploiting the flatness property of a simplified system to derive a feedback tracking law.

## 3. FLATNESS APPROACH

In this section, we simplify the dynamics of the original system (1)–(3) by assuming that  $a \gg 1$ , i.e. we neglect the inertia term at this boundary. The validity of this assumption will be discussed in Section 5 at the light of numerical simulations. Besides, we neglect the in-domain damping term, by assuming  $\lambda \ll 1$ . This yields the following system

$$u_{tt}(x, t) = u_{xx}(x, t) \quad x \in [0, 1], t > 0 \quad (6)$$

$$u_x(1, t) = U(t) \quad (7)$$

$$u_x(0, t) = -F(u_t(0, t)) \quad (8)$$

Our goal is to design a control law  $U(t)$  that exponentially stabilizes the following trajectory corresponding to a uniform rotation at constant speed  $\omega_r$

$$u_r(x, t) = a + \omega_r t + (1 - x)F(\omega_r), \quad U_r(t) = -F(\omega_r) \quad (9)$$

Besides we consider only a measurement of the top velocity

$$\omega(t) := u_t(1, t) \quad (10)$$

We design a dynamic output feedback controller using the flatness property of system (6)–(8) (see Laroche et al. (1998); Petit and Rouchon (2002)). In the sequel, we prove that  $z(t) = u(0, t)$  is the flat output of the system, before designing the stabilizing control law.

### 3.1 Flatness

In this section, we prove that system (6)–(8) is flat, i.e. its solutions can be parametrized by the output  $z(t) = u(0, t)$  and all its derivatives. The general solution of (6) is given by the d'Alembert formula

$$u(x, t) = \phi(t + x) + \psi(t - x) \quad (11)$$

where  $s \mapsto \phi(s)$  and  $s \mapsto \psi(s)$  are arbitrary functions corresponding to waves of velocity  $-1$  and  $1$ , respectively. Plugging this into the boundary conditions (7),(8) yields

$$U(t) = \phi'(t + 1) - \psi'(t - 1), \quad -F(\dot{z}(t)) = \phi'(t) - \psi'(t) \quad (12)$$

with  $z(t) = u(0, t) = \phi(t) + \psi(t)$ . Assume now that  $t \mapsto z(t)$  is known. The three above equations can be solved as follows

$$U(t) = \frac{\dot{z}(t + 1) - F(\dot{z}(t + 1))}{2} - \frac{\dot{z}(t - 1) + F(\dot{z}(t - 1))}{2} \quad (13)$$

$$\phi'(s) = \frac{\dot{z}(s) - F(\dot{z}(s))}{2}, \quad \psi'(s) = \frac{\dot{z}(s) + F(\dot{z}(s))}{2} \quad (14)$$

Thus

$$\phi(s) = a + \frac{z(s) - \int_0^s F(\dot{z}(\tau)) d\tau}{2} \quad (15)$$

$$\psi(s) = b + \frac{z(s) + \int_0^s F(\dot{z}(\tau)) d\tau}{2} \quad (16)$$

with  $a$  and  $b$  constants such that  $a + b = 0$  since  $z(t) = \phi(t) + \psi(t)$ . Coming back to the deformation profile  $u$ , we have the following parametrization

$$2u(x, t) = z(t + x) + z(t - x) - \int_{t-x}^{t+x} F(\dot{z}(\tau)) d\tau \quad (17)$$

This parametrization is explicit with respect to any arbitrary function  $t \mapsto z(t)$  corresponding to the bottom angle trajectory. There is a one-to-one correspondence between the solutions

of (6)–(8) and the flat output  $t \mapsto z(t)$ . Importantly, (17) shows that stabilizing the flat output is enough to stabilize the whole system.

### 3.2 Motion planning and tracking

In this section, we consider the problem of tracking any reference trajectory  $\omega_r(t)$  for the bottom velocity  $\dot{z}(t)$ . The corresponding reference control input can be deduced from (13), which yields

$$U(t) = \frac{w_r(t+1) - F(w_r(t+1))}{2} - \frac{w_r(t-1) + F(w_r(t-1))}{2} \quad (18)$$

However, for reference trajectories  $\omega_r$  where the derivative of  $F$  is positive, the system is unstable. Thus, the open-loop control (18) cannot be used. We now construct a global stabilizing controller around any reference  $t \mapsto \omega_r(t)$ . As will appear, the feedback depends solely on the top velocity measure  $\omega(t) = u_r(1, t)$ . The control design is summarized in the following theorem.

**Theorem 3.1.** The following control law

$$U(t) = -\omega(t) + v(t) - F(v(t)) \quad (19)$$

with

$$v(t) = \omega_r(t) - \lambda I(t) - \frac{\lambda}{2} \left( \int_{t-2}^t [v(\tau) + F(v(\tau))] d\tau \right), \quad (20)$$

$$\dot{I}(t) = \omega(t) - \omega_r(t) \quad (21)$$

exponentially stabilizes the reference trajectory  $\dot{z}(t) = \dot{u}_r(0, t) = \omega_r(t)$ . More precisely, we have

$$\frac{d}{dt} (\dot{z} - \omega_r) = -\lambda (\dot{z} - \omega_r) \quad (22)$$

**Proof** Differentiating (17) with respect to time and setting  $x = 1$  yields

$$\omega(t) = \frac{z(t+1) - F(\dot{z}(t+1))}{2} + \frac{z(t-1) + F(\dot{z}(t-1))}{2}$$

Along with (13), this yields

$$\omega(t) + U(t) = \dot{z}(t+1) - F(\dot{z}(t+1)).$$

Thus, setting

$$u(t) = -\omega(t) + v(t) - F(v(t))$$

where  $v(t)$  is a virtual control variable yields

$$\dot{z}(t+1) = v(t)$$

when the slope of  $F$  at  $v(t)$  is not equal to 1, i.e. when  $v \mapsto v - F(v)$  is locally a bijection. Interestingly, when  $dF/dv$  is close to 1, the system is strongly unstable. In particular, if  $F(v) = cv$  is a linear function, the eigenvalues of (6)–(8) tend to  $+\infty$  as  $c$  tends to 1 (see, e.g., Krstic (2009a)). Consider now a reference trajectory  $z_r(t+1)$  such that  $\dot{z}_r(t+1) = \omega_r(t)$ . Set

$$v(t) = \omega_r(t) - \lambda (z(t+1) - z_r(t+1)) \quad (23)$$

with  $\lambda > 0$ . Then, the closed-loop error dynamics read

$$\dot{y} - \dot{y}_r = -\lambda(y - y_r)$$

The problem is now to predict the future values  $z(t+1)$  from the measured output  $\omega$  and control  $u$  at times  $\leq t$ . Since  $\dot{z}(t) = v(t-1)$ , we have

$$z(t+1) = z(t-1) + \int_{t-2}^t v(\tau) d\tau \quad (24)$$

Plugging this into (17) at  $x = 1$  yields

$$\begin{aligned} u(1, t) &= z(t-1) + \frac{1}{2} \int_{t-2}^t v(\tau) d\tau - \frac{1}{2} \int_{t-1}^{t+1} F(\dot{z}(\tau)) d\tau \\ &= z(t-1) + \frac{1}{2} \int_{t-2}^t [v(\tau) - F(v(\tau))] d\tau \end{aligned}$$

Plugging this into (24)

$$z(t+1) = u(1, t) + \frac{1}{2} \int_{t-2}^t [v(\tau) + F(v(\tau))] d\tau$$

Thus, (23) now reads

$$\begin{aligned} v(t) &= \omega_r(t) - \lambda (u(1, t) - y_r(t+1)) \\ &\quad - \frac{\lambda}{2} \int_{t-2}^t [v(\tau) + F(v(\tau))] d\tau \end{aligned}$$

Finally, since  $\dot{z}_r(t+1) = \omega_r(t)$  and  $u_r(1, t) = \omega(t)$ , we can compute  $u(1, t) - y_r(t+1)$  as an error integral

$$I := u(1, t) - y_r(t+1), \quad \dot{I}(t) = \omega(t) - \omega_r(t). \quad (25)$$

which yields (19)–(21).

## 4. BACKSTEPPING APPROACH

In this section, we derive a backstepping controller (see, e.g. Smyshlyaev and Krstic (2009)) based on a different simplification of the original system. We linearize the boundary condition (3) around a reference trajectory of the form (4)–(5) for a given reference velocity  $\omega_r$ , while keeping the in-domain damping and the drill bit inertia terms. The linearized equations read

$$u_{tt}(x, t) = u_{xx}(x, t) - \lambda u_t(x, t), \quad x \in [0, 1], t > 0 \quad (26)$$

$$u_x(1, t) = U(t) \quad (27)$$

$$u_{tt}(0, t) = au_x(0, t) + abu_t(0, t) \quad (28)$$

where  $b = \frac{\partial F}{\partial \omega}(\omega_r)$ . For  $b > 0$ , the zero equilibrium of (26)–(28) is unstable. We now propose a control law that makes the zero equilibrium of (26)–(28) exponentially stable in the sense of an appropriate norm. To do so, we consider the following alternate set of state variables

$$v(x, t) = \frac{\partial(u - \bar{u})}{\partial x}(x, t), \quad y(t) = u_t(0, t), \quad V(t) = U(t) - \bar{U}$$

This yields the following coupled PDE-ODE system

$$v_{tt}(x, t) = v_{xx}(x, t) - \lambda v_t(x, t), \quad x \in [0, 1] \quad (29)$$

$$v(1, t) = V(t) \quad (30)$$

$$v_x(0, t) = av(0, t) + (\lambda + ab)y(t) \quad (31)$$

$$\dot{y}(t) = aby(t) + av(0, t) \quad (32)$$

Our goal is to design a control law  $V(t)$  that exponentially stabilizes the zero equilibrium of the whole system (29)–(32). To do so, we map the system to a target system with desirable stability properties using a backstepping transformation. Sufficient conditions on the transformation kernels, taking the form of wave PDEs on a triangular domain, are derived and solved. This results in a full-state feedback law yielding exponential stability of the zero equilibrium in an appropriate norm.

### 4.1 Target system

The target system equations read

$$w_{tt}(x, t) = w_{xx}(x, t) - \lambda w_t(x, t), \quad x \in [0, 1] \quad (33)$$

$$w(1, t) = 0 \quad (34)$$

$$w_x(0, t) = cw_t(0, t) \quad (35)$$

$$\dot{y}(t) = -\delta y(t) + aw(0, t) \quad (36)$$

where  $c$  and  $\delta$  are strictly positive design parameters.

*Lemma 4.1.* (Stability of the target system). The zero equilibrium of (33)–(36) is exponentially stable in the sense of the following system norm

$$\Gamma(t) = \left( \|w_x(\cdot, t)\|_{\mathcal{L}^2([0,1])} + \|w_t(\cdot, t)\|_{\mathcal{L}^2([0,1])} + |y(t)| \right)^{1/2} \quad (37)$$

**Proof** We consider the following candidate Lyapunov function

$$\begin{aligned} \Omega(t) = & \frac{1}{2} \int_0^1 w_x^2 dx + \frac{1}{2} \int_0^1 w_t^2 dx \\ & + \epsilon \int_0^1 (-2+x) w_t w_x dx + \frac{1}{2} \beta y(t)^2 \end{aligned} \quad (38)$$

where  $\beta$  and  $\epsilon$  are strictly positive analysis parameters. We have omitted the space and time arguments when the notation is obvious, i.e.  $\int_0^1 w_x^2 dx$  stands for  $\int_0^1 w_x(x, t)^2 dx$ . For  $\beta$  small enough, there exists  $m_1, m_2 > 0$  such that<sup>4</sup>

$$m_1 \Gamma^2 \leq \Omega \leq m_2 \Gamma^2 \quad (39)$$

The time derivative of  $\Omega$  reads

$$\begin{aligned} \dot{\Omega}(t) = & \int_0^1 w_{tx} w_x dx + \int_0^1 w_{tt} w_t dx + \epsilon \int_0^1 (-2+x) w_t w_{tx} dx \\ & + \epsilon \int_0^1 (-2+x) w_{tt} w_x dx - \delta \beta y(t)^2 + a \beta y(t) w(0) \end{aligned}$$

Using Young's inequality on the last term, with a parameter  $d > 0$ , yields

$$\begin{aligned} \dot{\Omega}(t) = & -c w_t(0)^2 - \lambda \int_0^1 \left[ w_t^2 + \epsilon (-2+x) w_t w_x \right] dx \\ & - \frac{\epsilon}{2} \int_0^1 \left( w_t^2 + w_x^2 \right) dx - \frac{\epsilon}{2} \left[ w_t(1)^2 + w_x(1)^2 \right] \\ & + \epsilon \left[ w_t(0)^2 + w_x(0)^2 \right] - \delta \beta y(t)^2 + \frac{d}{2} a \beta^2 y(t)^2 + \frac{a}{2d} w(0)^2 \end{aligned}$$

Using Agmon's inequality along with Poincaré's inequality for the last term, and setting  $\epsilon < \frac{c}{1+c^2}$  yields

$$\begin{aligned} \dot{\Omega}(t) \leq & -\frac{\epsilon}{2} \int_0^1 w_t^2 dx - \left[ \frac{\epsilon}{2} - \frac{\epsilon^2}{2} - \frac{2a}{d} \right] \int_0^1 w_x^2 dx \\ & - \beta \left[ \delta - \frac{\alpha \beta d}{2} \right] y(t)^2 \end{aligned} \quad (40)$$

which is negative definite for

$$\epsilon < 1, \quad d > \frac{4a}{\epsilon(1-\epsilon)}, \quad \beta < \frac{2\delta}{\alpha d}$$

Thus, it follows from (38),(39) and (40) that

$$\Gamma(t) \leq M e^{-t/M} \Gamma(0) \quad (41)$$

for some  $M > 0$ , which concludes the proof.

In the next section, we define a transformation that maps the original system (29)–(32) to the target system (33)–(36).

#### 4.2 Backstepping transformation

In order to match system (29)–(32) to the target system (33)–(36), we consider the following transformation  $(y, v, v_t) \mapsto (y, w, w_t)$

$$\begin{aligned} w(x, t) = & v(x, t) - \int_0^x k(x, \xi) v(\xi, t) d\xi \\ & - \int_0^x s(x, \xi) v_t(\xi, t) d\xi - \gamma(x) y(t) \end{aligned} \quad (42)$$

<sup>4</sup> This result can be proved using the Cauchy-Schwarz and Young's inequalities Krstic and Smyshlyaev (2008).

where  $k, s$  and  $\gamma$  are yet to be determined. The kernels  $k$  and  $s$  are defined on the triangular domain  $\mathcal{T} = \{(x, \xi) \mid 0 \leq \xi \leq x \leq 1\}$ , whereas  $\gamma$  is defined on  $[0, 1]$ . Plugging transformation (42) into (33) and using (29),(31),(32) yields, after a lengthy but straightforward computation

$$\begin{aligned} 0 = & w_{tt}(x, t) - w_{xx}(x, t) + \lambda w_t(x, t) \\ = & \int_0^x [k_{xx} - k_{yy}] v(\xi, t) d\xi + \int_0^x [s_{xx} - s_{yy}] v_t(\xi, t) d\xi \\ & + 2 \frac{d}{dx} k(x, x) v(x, t) + 2 \frac{d}{dx} s(x, x) v_t(x, t) \\ & + [ak(x, 0) - k_\xi(x, 0) + a(\lambda + ab)(s(x, 0) - \gamma(x))] v(0, t) \\ & + [as(x, 0) - s_\xi(x, 0) - a\gamma(x)] v_t(0, t) \\ & + [(\lambda + ab)(k(x, 0) + abs(x, 0) - ab\gamma(x)) - \gamma''(x)] y(t) \end{aligned} \quad (43)$$

Besides, plugging the transformation (42) into (35) and using (31),(32) yields

$$\begin{aligned} 0 = & w_x(0, t) - c w_t(0, t) \\ = & [a + ac\gamma(0) - k(0, 0)] v(0, t) - [s(0, 0) + c] v_t(0, t) \\ & + [\lambda + ab - \gamma'(0) + abc\gamma(0)] \end{aligned} \quad (44)$$

Also, plugging the transformation into (36) and using (32) yields

$$0 = [ab + \delta + a\gamma(0)] y(t) \quad (45)$$

Finally, plugging (42) into (34) imposes the following control law

$$V(t) = \int_0^1 k(1, \xi) v(\xi, t) + \int_0^1 s(1, \xi) v_t(\xi, t) + \gamma(1) y(t) \quad (46)$$

Thus, a sufficient condition for (43)–(45) to hold for all  $v(x, t), v_t(x, t), y(t)$  is that the kernels  $k, s$  and  $\gamma$  satisfy the following set of equations

$$\left\{ \begin{aligned} k_{xx}(x, \xi) &= k_{\xi\xi}(x, \xi), & \frac{d}{dx} k(x, x) &= 0, \\ s_{xx}(x, \xi) &= s_{\xi\xi}(x, \xi), & \frac{d}{dx} s(x, x) &= 0, \\ \gamma''(x) &= (\lambda + ab) [k(x, 0) + abs(x, 0) - ab\gamma(x)], \\ k_\xi(x, 0) &= ak(x, 0) + a(\lambda + ab) [s(x, 0) - \gamma(x)], \\ s_\xi(x, 0) &= as(x, 0) - a\gamma(x), \\ k(0, 0) &= a - c(ab + \delta), \\ s(0, 0) &= -c, \\ \gamma'(0) &= \lambda + ab - (ab + \delta)bc, \\ a\gamma(0) &= -ab - \delta \end{aligned} \right. \quad (47)$$

System (47) can be solved explicitly, as follows

$$k(x, \xi) = \kappa(x - \xi), \quad s(x, \xi) = \sigma(x - \xi) \quad (48)$$

$$\begin{pmatrix} \kappa(s) \\ \sigma(s) \\ \gamma(s) \\ \gamma'(s) \end{pmatrix} = e^{Ms} \begin{pmatrix} a - c(ab + \delta) \\ -c \\ -b - \delta/a \\ (\lambda + ab - (ab + \delta)bc) \end{pmatrix},$$

$$M = \begin{pmatrix} -a & -a(\lambda + ab) & a(\lambda + ab) & 0 \\ 0 & -a & a & 0 \\ 0 & 0 & 0 & 1 \\ \lambda + ab & ab(\lambda + ab) & -ab(\lambda + ab) & 0 \end{pmatrix} \quad (49)$$

#### 4.3 Inverse transformation

Because of the damping term in the target system boundary condition (35), one must consider the following inverse transformation  $(y, w, w_t, w_x) \mapsto (y, v, v_t, v_x)$

$$v(x, t) = w(x, t) - \int_0^x m(x, \xi)w(\xi, t)d\xi - \int_0^x n(x, \xi)w_t(\xi, t)d\xi - \int_0^x p(x, \xi)w_x(\xi, t)d\xi - \rho(x)y(t) \quad (50)$$

The kernels satisfy the following system of equations

$$\begin{cases} m_{xx}(x, \xi) = m_{\xi\xi}(x, \xi), & \frac{d}{dx}m(x, x) = 0, \\ n_{xx}(x, \xi) = n_{\xi\xi}(x, \xi), & \frac{d}{dx}n(x, x) = 0, \\ p_{xx}(x, \xi) = p_{\xi\xi}(x, \xi), & \frac{d}{dx}p(x, x) = 0, \\ \rho''(x) = [\delta^2 + \delta a - \lambda\delta]\rho(x), & \rho(x, 0) = -cn(x, 0), \\ n_\xi(x, 0) = cm(x, 0) - cp_\xi(x, 0) - \lambda cn(x, 0) - a\rho(x), & m_\xi(x, 0) = -a(\lambda + \delta)\rho(x), \\ m(0, 0) = -a, & n(0, 0) = c[1 - p(0, 0)], \\ \rho'(0) = \delta - \lambda, & a\rho(0) = \delta + ab \end{cases} \quad (51)$$

Again, this system can be solved explicitly as follows

$$\begin{aligned} m(x, \xi) &= \mu(x - \xi), & n(x, \xi) &= \eta(x - \xi), \\ p(x, \xi) &= -c\eta(x - \xi) \end{aligned} \quad (52)$$

$$\begin{pmatrix} \mu(s) \\ \eta(s) \\ \rho(s) \\ \rho'(s) \end{pmatrix} = e^{Ns} \begin{pmatrix} -a \\ c \\ \frac{1+c^2}{b+\delta/a} \\ \delta - \lambda \end{pmatrix},$$

$$N = \begin{pmatrix} 0 & 0 & a(\lambda + \delta) & 0 \\ c & -\lambda c & -a & 0 \\ c^2 - 1 & c^2 - 1 & c^2 - 1 & 0 \\ 0 & 0 & 0 & 1 \\ 0 & 0 & \delta^2 + \delta a - \lambda\delta & 0 \end{pmatrix} \quad (53)$$

#### 4.4 Control law

**Theorem 4.2.** Consider system (29)–(32) with the control law (46) where  $k$ ,  $s$  and  $\gamma$  are defined by (48)–(49). The equilibrium  $(v, y) \equiv (0, 0)$  is exponentially stable in the sense of the following system norm

$$\Xi(t) = \left( \|v(\cdot, t)\|_{\mathcal{L}^2([0,1])} + \|v_x(\cdot, t)\|_{\mathcal{L}^2([0,1])} + \|v_t(\cdot, t)\|_{\mathcal{L}^2([0,1])} + |y(t)|^2 \right)^{1/2} \quad (54)$$

**Proof** Differentiating (42) with respect to time, using (29),(46) and integrating by parts yields

$$\begin{aligned} w_t(x) &= v_t(x) - s(x, x)v_x(x) - \int_0^x [k(x, \xi) - \lambda s(x, \xi)]v_t(\xi)d\xi \\ &+ s_\xi(x, 0) \left[ \int_0^1 v_x(\xi)d\xi + \int_0^1 k(1, \xi)v(\xi)d\xi + \int_0^1 s(1, \xi)v_t(\xi)d\xi \right] \\ &+ \int_0^x s_\xi(x, \xi)v_x(\xi)d\xi + [\gamma(1)s_\xi(x, 0) - abs(x, 0)]y(t) \end{aligned} \quad (55)$$

Similarly, differentiating (42) with respect to  $x$  yields

$$\begin{aligned} w_x(x) &= v_x(x) - k(x, x)v(x) - \int_0^x k_x(x, \xi)v(\xi)d\xi \\ &- s(x, x)v_t(x) - \int_0^x s_x(x, \xi)v_t(\xi)d\xi - \gamma'(x)y(t) \end{aligned} \quad (56)$$

By using Cauchy-Schwarz's inequality, it is thus possible to show that there exists  $\theta_1 > 0$  such that

$$\Gamma(t) \leq \theta_1 \Xi(t) \quad (57)$$

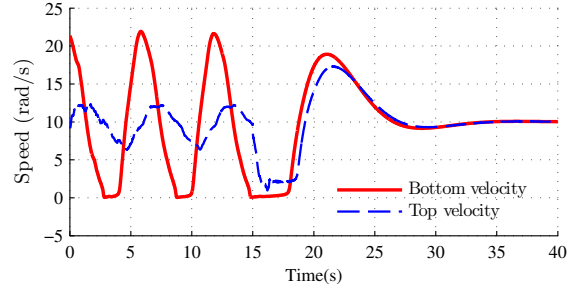


Fig. 3. Stabilization of the drilling using the flatness controller (19)–(21). The controller is turned on after 15 seconds.

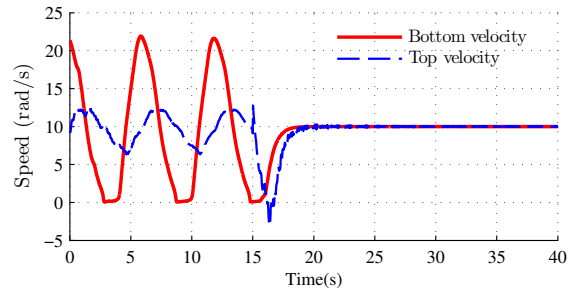


Fig. 4. Stabilization of the drilling using the backstepping controller (46). The controller is turned on after 15 seconds.

Similarly, using the inverse transformation (50), and Cauchy-Schwarz's, Agmon's and Poincaré's inequalities, one can show that

$$\Xi(t) \leq \theta_2 \Gamma(t) \quad (58)$$

for some  $\theta_2 > 0$ . Combining (41),(57),(58) yields

$$\Xi(t) \leq M\theta_1\theta_2 e^{-t/M}\Xi(0) \quad (59)$$

which concludes the proof. In the next section, the performances of both the flatness and the backstepping controllers are tested in numerical simulations.

## 5. NUMERICAL SIMULATIONS

### 5.1 Stabilization results

In this section, we present numerical simulations illustrating the merits and drawbacks of the controllers (19)–(21) and (46), respectively. The system described in Saldivar et al. (2011) is used as the simulation model. It is equivalent to (1)–(3), as illustrated in Appendix, but is expressed in the physical coordinates, which eases the interpretation of the results, and comparison with previous control solutions. Figure 3 pictures a stabilization of the drillstring using the flatness controller (19),(21). Figure 4 pictures a stabilization of the drillstring using the backstepping controller (46). Both controllers were turned on at  $t = 15$  s., in the stick phase.

### 5.2 Discussion

The backstepping controller immediately suppresses any velocity oscillation and features a settling time which is at least five times lower than for the flatness controller, or other approaches, such as Canudas-de Wit et al. (2008) and Serrarens et al. (1998). However, it uses full-state feedback, which is not

Symbol	Description	Value
$L$	Length of the drillpipe	2000 m
$I_d$	Inertia of the drillpipe per unit length	0.095 kg m
$I_b$	Inertia of the BHA	311 kg m <sup>2</sup>
$G$	Shear modulus	79.3 · 10 <sup>9</sup> N/m <sup>2</sup>
$J$	Geometric moment of inertia	1.19 · 10 <sup>-5</sup> m <sup>4</sup>
$\beta$	Drillstring damping	0 kg m/s
$T_{\text{robdyn}}$	Friction parameter	7500 N
$\alpha_1, \alpha_2, \alpha_3$	Friction parameters	5.5; 2.2; 3500
$c_b$	Viscous damping torque at the bit	0.03 Nm s/rad

Table 1. List of the parameters used

realistic in practice. In order to implement it on an actual drillstring, one needs to design a boundary observer using topside measurements only. Observers for similar systems are derived in Smyshlyaev and Krstic (2009); Krstic (2009b) but we could not directly extend these designs to the dynamics (26)–(28). In turn, the flatness controller tends to overshoot as pictured in Figure 3. The reason for this is that the assumption  $a \gg 1$ , which amounts to neglecting the bit inertia is actually not valid for the considered case (see Table 1). Unfortunately, even though retaining the bit inertia does not suppress the flatness property of the system, we could not obtain the closed-form expression (17) when replacing the boundary condition (8) by the original boundary condition (28). To further assess the performances of these controllers, it is crucial to evaluate their robustness to changes in operating conditions, such as variations of the weight-on-bit. This, along with the design of an observer for the backstepping controller, will be topic of future investigations.

## REFERENCES

- A.G. Balanov, N.B. Janson, P.V.E. McClintock, R.W. Tucker, and C.H.T. Wang. Bifurcation analysis of a neutral delay differential equation modelling the torsional motion of a driven drill-string. *Chaos, Solitons & Fractals*, 15(2): 381 – 394, 2003. ISSN 0960-0779.
- C. Canudas-de Wit, F.R. Rubio, and M.A. Corchero. D-oskil: A new mechanism for controlling stick-slip oscillations in oil well drillstrings. *Control Systems Technology, IEEE Transactions on*, 16(6):1177–1191, nov. 2008.
- M. Fliess, J. Lévine, P. Martin, and P. Rouchon. On differentially flat nonlinear systems. In *IFAC SYMPOSIA SERIES*, pages 159–163. Pergamon Press, 1993.
- J. D. Jansen. *Nonlinear dynamics of oilwell drillstrings*. PhD thesis, Delft University of Technology, 1993.
- J.D. Jansen and L. van den Steen. Active damping of self-excited torsional vibrations in oil well drillstrings. *Journal of Sound and Vibration*, 179(4):647 – 668, 1995. ISSN 0022-460X.
- M. Krstic. Adaptive control of an anti-stable wave pde. In *American Control Conference, 2009. ACC '09.*, pages 1505–1510, june 2009a.
- M. Krstic. Compensating a string pde in the actuation or sensing path of an unstable ode. In *American Control Conference, 2009. ACC '09.*, pages 4097–4102, june 2009b.
- M. Krstic and A. Smyshlyaev. Backstepping boundary control for first-order hyperbolic pdes and application to systems with actuator and sensor delays. *Systems & Control Letters*, 57(9):750 – 758, 2008. ISSN 0167-6911.
- B. Laroche, P. Martin, and P. Rouchon. Motion planning for a class of partial differential equations with boundary control. In *Decision and Control, 1998. Proceedings of the 37th IEEE Conference on*, volume 3, pages 3494–3497 vol.3, 1998.
- E.M. Navarro-Lopez and D. Cortes. Sliding-mode control of a multi-dof oilwell drillstring with stick-slip oscillations. In *American Control Conference, 2007. ACC '07*, pages 3837–3842, july 2007.
- N. Petit and P. Rouchon. Flatness of heavy chain systems. In *Decision and Control, 2002, Proceedings of the 41st IEEE Conference on*, volume 1, pages 362 – 367 vol.1, dec. 2002.
- M. B. Saldivar, S. Mondie, J.-J. Loiseau, and V. Rasvan. Stick-Slip Oscillations in Oilwell Drillstrings: Distributed Parameter and Neutral Type Retarded Model Approaches. *Proceedings of the 18th IFAC World Congress*, 18:284–289, 2011.
- A.F.A. Serrarens, M.J.G. van de Molengraft, J.J. Kok, and L. van den Steen.  $\mathcal{H}^\infty$  control for suppressing stick-slip in oil well drillstrings. *IEEE Control Systems*, 18(2):19–30, apr 1998. ISSN 1066-033X.
- A. Smyshlyaev and M. Krstic. Boundary control of an anti-stable wave equation with anti-damping on the uncontrolled boundary. In *American Control Conference, 2009. ACC '09.*, pages 1511–1516, june 2009.
- Qizhi Zhang, Yu yao He, Lin Li, and Nurzat. Sliding mode control of rotary drilling system with stick slip oscillation. In *Intelligent Systems and Applications (ISA), 2010 2nd International Workshop on*, pages 1–4, may 2010.

## Appendix A. DESCRIPTION OF THE PHYSICAL MODEL

In Saldivar et al. (2011), the torsional dynamics of the drilling systems are modelled as follows

$$GJ\theta_{\xi\xi}(\xi, \tau) - I_d\theta_{\tau\tau}(\xi, \tau) - \beta\theta_\tau(\xi, \tau) = 0, \\ \xi \in [0, L], \tau > 0 \quad (\text{A.1})$$

with boundary conditions

$$GJ\theta_\xi(0, \tau) = c_a(\theta_\tau(0, \tau) - \Omega(\tau)) \quad (\text{A.2})$$

$$GJ\theta_\xi(L, \tau) + I_b\theta_{\tau\tau}(L, \tau) = -T(\theta_\tau(L, \tau)) \quad (\text{A.3})$$

where  $\theta(\xi, \tau)$  is the angle of rotation. At the surface, the drillstring is rotated by a rotor with angular velocity  $\Omega(t)$ . The bottom boundary condition (A.3) features an inertia term  $I_b\theta_{\tau\tau}(L, \tau)$  corresponding to the Bottom Hole Assembly and a friction term  $T(\theta_\tau(L, \tau))$ . The function  $T$ , modelling dry friction and viscous damping at the bit, has the following expression, following Zhang et al. (2010)

$$T(\omega) = c_b\omega + T_{\text{obdyn}}\frac{2}{\pi}(\alpha_1\omega e^{-\alpha_2|\omega|} + \text{atan}(\alpha_3\omega)) \quad (\text{A.4})$$

To ease the numerical simulation, it is a smoothed approximation of the bit-rock interaction model used in Saldivar et al. (2011). The physical parameters are listed in Table 1. They are representative of a standard drilling system and are taken from Jansen and van den Steen (1995). In order to improve clarity, we have considered the following variable change

$$u(x, t) = \theta\left(L(1-x), L\sqrt{\frac{I_d}{GJ}}t\right) \quad (\text{A.5})$$

which yields system (1)–(3) where we have set

$$\lambda = L\beta\sqrt{\frac{1}{GJ I_d}}, \quad a = L\frac{I_d}{I_b} \quad (\text{A.6})$$

$$U(t) = \frac{L}{GJ}c_a\left(\Omega(t) - \frac{1}{L}\sqrt{\frac{GJ}{I_d}}u_t(1, t)\right) \quad (\text{A.7})$$

$$F(\omega) = -\frac{L}{GJ}T\left(\frac{1}{L}\sqrt{\frac{GJ}{I_d}}\omega\right) \quad (\text{A.8})$$